

Article

Effects of Different Antioxidant Intercalated Layered Double Hydroxides on Anti-Aging Properties of Asphalt Binders

Quantao Liu *, Jinjie Li and Shuaichao Chen

State Key Laboratory of Silicate Materials for Architectures, Wuhan University of Technology, Wuhan 430070, China; chensc@whut.edu.cn (S.C.)

* Correspondence: liuqt@whut.edu.cn

Abstract: This research aims to prepare different antioxidant intercalated layered double hydroxides (LDHs) and compare the thermal oxidation and ultraviolet (UV) aging resistances of different modified asphalts. The ion exchange technique was used to intercalate three different antioxidants: 3-(3,5-di-tert-butyl-4-carboxyphenyl) propionic acid, antioxidant 1222, and sodium dibutyl dithiocarbamate (rubber accelerator TP) into the interlayer of LDHs. The morphology, structures, UV blocking, and free radical scavenging properties of different antioxidant intercalated LDHs were characterized, respectively. The effects of the anti-aging agents on the physical properties (penetration, softening point, ductility, and viscosity); rheological behaviors (complex modulus and phase angle); and functional groups (C=O and S=O) of asphalt both before and after thermal oxidation aging and UV aging were systematically investigated. The results of the crystal structure and functional group analysis show that the three different antioxidants can be successfully inserted into the interlayer of LDHs without destroying their layered structures. Antioxidant intercalated LDHs exhibit a remarkable capacity for absorbing UV rays, coupled with a moderate ability to reflect UV light. Moreover, the inclusion of antioxidants into the interlayers of LDHs confers upon them the ability to scavenge free radicals. After 2 h of reaction, the free radical scavenging rates of LDHs-3, LDHs-1222, and LDHs-TP were 57.7%, 35.6%, and 17.1%, respectively. With an increase in the content of the antioxidant intercalated LDHs, the performance of the modified asphalt varies, and 4% is the optimal content of the anti-aging agents. Asphalts with the three antioxidant intercalated LDHs all had favorable storage stability, and their physical and rheological properties were improved after aging compared to LDHs-modified asphalt. The LDHs-3-modified asphalt showed the best anti-ultraviolet aging effect, while LDHs-1222-modified asphalt showed the best anti-thermal oxidation aging effect. This research lays the foundation for developing aging-resistant asphalt and improving the durability of asphalt pavement.

Keywords: asphalt; antioxidant intercalated LDHs; free radical scavenging property; UV aging resistance; thermal oxidation aging resistance



Citation: Liu, Q.; Li, J.; Chen, S. Effects of Different Antioxidant Intercalated Layered Double Hydroxides on Anti-Aging Properties of Asphalt Binders. *Buildings* **2024**, *14*, 593. <https://doi.org/10.3390/buildings14030593>

Academic Editor: Rui Xiao

Received: 9 January 2024

Revised: 18 February 2024

Accepted: 21 February 2024

Published: 23 February 2024



Copyright: © 2024 by the authors. Licensee MDPI, Basel, Switzerland. This article is an open access article distributed under the terms and conditions of the Creative Commons Attribution (CC BY) license (<https://creativecommons.org/licenses/by/4.0/>).

1. Introduction

Asphalt is susceptible to aging due to the influence of external conditions such as high temperature, oxygen, and ultraviolet light [1,2]. During processing, storage, transportation, mixing, and paving, high temperatures can cause asphalt molecules to undergo dehydrogenation, oxygen absorption, and polycondensation reactions [3], resulting in severe thermal oxidation aging of asphalt binders in a short time. Additionally, the light components in the asphalt tend to evaporate quickly at high temperatures, increasing the proportion of heavier components and lowering the asphalt performance [4]. During service, asphalt pavement absorbs infrared light and electromagnetic radiation, resulting in an increase in pavement temperature and causing long-term thermal oxidation aging of asphalt [5]. Asphalt thermal oxidation aging is a chain reaction [6]. Under the influence of high temperatures and oxygen, alkyl hydrocarbon bonds in asphalt break to form free

radicals [7,8]. These free radicals then interact with the active groups in the asphalt to produce new free radicals and intermediate products [9]. The intermediate products can decompose into new free radicals or react with C=C of asphalt to form carboxyl groups, which causes the deepening of asphalt aging over time [10].

Asphalt is also subjected to UV aging during service [11]. High-energy UV light will cause some chemical bonds in asphalt to break, create free radicals, and start the chain reaction [12]. Malinowski [13] studied the aromatization process of asphalt due to UV radiation and explored how the aromatization process affected the electronic structures of asphalt components and promoted the aging of asphalt. The results show that the aromatization reaction of asphaltene is the most favorable in energy, and the significant increase in the polarity of saturated compounds due to aromatization is conducive to the formation of cracks in asphalt pavements. Hu et al. [14] investigated the effect of various bands of UV light on the performance of asphalt and found that the UV light of the 300–350 nm bands had the greatest aging effect on asphalt. Zeng et al. [15] studied the aging depth of asphalt by UV spectrophotometry and the stripping method. The findings demonstrated that ultraviolet radiation can only age the asphalt for a limited depth of 4.5 μm , and the aging phenomenon below this depth was mainly caused by the diffusion of the aged asphalt at the surface. Wu et al. [16] collected asphalt materials that have been aged in the field for 10 years and subsequently measured their aging indices. The findings indicated that UV aging of the asphalt pavement was severe. Aged asphalt will become hard and brittle, prone to potholes and cracks, seriously affecting the service life of asphalt pavement [17].

The service life of asphalt pavement is directly impacted by the durability of asphalt [18]. Therefore, enhancing asphalt's anti-aging properties is crucial for increasing the service life of asphalt pavement [19]. Adding antioxidants, silicate materials, inorganic nanoparticles, organic UV absorbers, layered double hydroxides (LDHs), etc. can enhance the anti-aging performance of asphalt. Wu et al. [20] inhibited the increase in viscosity, softening point, carbonyl index, and sulfoxide index of asphalt during short-term thermal oxidation aging and pressure aging by incorporating antioxidant Irganox 1010, which effectively improved the thermal-oxidation aging resistance of asphalt. Ouyang et al. [21] added 1% antioxidant ZDDP to the base asphalt and proved that the modified asphalt had good thermal oxidation aging resistance. However, the anti-aging effects of antioxidants are not long-lasting, because they will react with asphalt radicals and gradually lose their effectiveness. The layered silicate materials such as montmorillonite and expanded vermiculite have a blocking effect on heat and oxygen and are often used to improve the anti-aging performance of asphalt. Liu et al. [22] and Wang et al. [23] found that nano-montmorillonite can form a peeling or intercalation structure to hinder the penetration of heat and oxygen into asphalt, thereby improving the thermal oxidation aging resistance of asphalt. Zhang et al. [24,25] reported that adding expanded vermiculite into asphalt and peeling it into a nanostructure in the asphalt can hinder the volatilization of asphalt light components, inhibit the penetration of oxygen into asphalt, and thus enhance its thermal oxidation aging resistance. However, inorganic layered silicate materials have poor compatibility with asphalt and have a limited effect on improving the UV aging resistance of asphalt.

The UV aging resistance of asphalt can be enhanced by incorporating UV-absorbing materials such as nano- Ce_2O_3 , nano- ZnO , and nano- TiO_2 , which absorb UV light and convert it into heat, visible light, etc. Zhang et al. [26] successfully used nano- TiO_2 , CeO_2 , and carbon black to enhance the anti-UV aging properties of asphalt used in the Tibetan Plateau. However, these inorganic nanomaterials have poor compatibility with asphalt and inferior resistance to thermal oxidation aging. Xu et al. [27] found that adding organic UV-absorbing materials UV326, UV531, and UV770 can also improve the UV aging performance of asphalt by converting UV damage into heat, but these organic UV absorbers will produce structural changes and thus gradually fail after absorbing UV rays. LDHs are an inorganic functional material made up of an interlayer guest anion and a host bimetallic hydroxide layer [28]. Their unique layered structure can shield UV light, and the metal cations on the layers and the interlayer anions can absorb UV light to some extent, thus enhancing the

anti-UV aging performance of asphalt [29]. However, there are many hydroxyl groups on the surface of LDH laminates, which make them hydrophilic and have poor compatibility with asphalt. Using the exchangeable characteristics of interlayer anions of LDHs, organic anion intercalation was carried out to improve its compatibility with asphalt [30]. Xu et al. [31] intercalated organic anions into the interlayer of LDHs, preparing organic-modified LDHs. The results showed that the intercalated LDHs had good compatibility with asphalt and improved the anti-aging performance of the modified asphalt. However, LDHs cannot effectively enhance the thermal oxidation aging resistance of asphalt. How to simultaneously enhance the thermal oxidation and UV aging resistances of asphalt is a still big challenge for researchers.

Chen et al. [32] intercalated the antioxidant into the interlayer of LDHs and simultaneously improved the thermal oxidation and UV aging resistances of asphalt binders, making it a very promising anti-aging material. However, only one antioxidant was studied in this research, and the antioxidant intercalated LDHs have not been optimized. As antioxidants have selectivity in capturing free radicals, it is of great importance to study the anti-thermal oxidation aging and anti-UV aging effects of different antioxidant intercalated LDHs on asphalt binders.

This paper aims to prepare different antioxidants intercalated LDHs and compare their effects on the thermal oxidation aging and UV aging resistances of asphalt. LDHs with different antioxidants intercalated were prepared using the ion exchange method and were used to modify asphalt. The antioxidant intercalated LDHs were characterized by a X-ray diffractometer (XRD), Fourier-Transform infrared spectroscopy (FTIR), a scanning electron microscope (SEM), and a ultraviolet spectrophotometer (UV-Vis), and the physical and rheological properties, aging index, and anti-aging effectiveness of several modified asphalts were evaluated by comparing their properties before and after thermal oxidation aging and UV aging.

2. Experiments

2.1. Materials

LDHs with a Mg/Al molar ratio of 2.0 were obtained from the Beijing University of Chemical Technology. Antioxidant 3-(3,5-di-tert-butyl-4-carboxyphenyl) propionic acid with purity 98%, chemical formula $C_{17}H_{26}O_3$, and a relative molecular mass of 278.39 was purchased from Guangdong Wengjiang Chemical Reagent Co., Ltd, Guangdong, China. Antioxidant 1222 with purity 98%, chemical formula $C_{19}H_{33}O_4P$, and a relative molecular mass of 356.44 was bought from Beijing Guoyao Chemical Reagent Co., Ltd., Beijing, China. The antioxidant sodium dibutyl dithiocarbamate (rubber accelerator TP) was obtained from Guangdong Wengjiang Chemical Reagent Co., Ltd., which was analytically pure, with a chemical formula of $C_9H_{18}NNaS_2$ and a relative molecular mass of 227.37. These antioxidants were referred to as antioxidant 3, antioxidant 1222, and antioxidant TP. The free radical DPPH (1,1-diphenyl-2-picrylhydrazyl) with a chemical formula of $C_{18}H_{12}N_5O_6$ was purchased from Pharmaceutical Group Chemical Reagents Co., Ltd., Shanghai, China. Deionized water and anhydrous ethanol were obtained in the laboratory. The asphalt used in the experiment was penetration grade 70# petroleum asphalt produced by Hubei Guochuang High-tech Materials Co., Ltd., Wuhan, China, and its properties as shown in Table 1 meet the requirements of the Technical Specifications for Construction of Highway Asphalt Pavement JTG F40-2004 [33].

Table 1. Physical properties of the penetration grade 70# petroleum asphalt.

Physical Property	Unit	Required Value	Test Result
Penetration (25 °C)	dmm	60~80	72.7
Softening point	°C	≥46	48.3
Ductility (10 °C)	cm	≥15	19.2
Viscosity (60 °C)	Pa. s	≥180	284

2.2. Preparation and Characterization of Antioxidant Intercalated LDHs

2.2.1. Preparation of Antioxidant Intercalated LDHs

In this paper, antioxidant intercalated LDHs were prepared by the ion exchange method. A schematic diagram of the synthesis of LDHs antioxidants is shown in Figure 1. The specific steps are as follows: (1) A 500 mL three-necked flask was filled with 100 mL of deionized water and 100 mL of anhydrous ethanol, and the water–ethanol solvent was obtained by stirring. Then, 10.0 g LDHs was added to the mixed solvent, heated to 60 °C, and stirred for 1 h to obtain LDHs slurry. (2) A certain amount of antioxidant (9.2 g antioxidant 3, 11.8 g antioxidant 1222, and 7.5 g antioxidant TP) was added to 100 mL deionized water, and the antioxidant solution was obtained after full stirring. (3) The prepared antioxidant intercalation solution was added to the LDHs slurry, then the nitrogen protection was introduced, and the solution was stirred and refluxed at 60 °C for 5 h to complete the intercalation. (4) The antioxidant intercalated LDHs slurry was filtered and repeatedly washed with deionized water to produce the filter cake by reduced pressure filtration after the reaction was finished and the solution had cooled to room temperature. Then, the filter cake was dried in a vacuum-drying oven at 70 °C for 24 h. The filter cake was removed and ground to obtain the antioxidant intercalated LDHs. The LDHs after intercalation of the three antioxidants were noted as LDHs-3, LDHs-1222, and LDHs-TP, respectively.

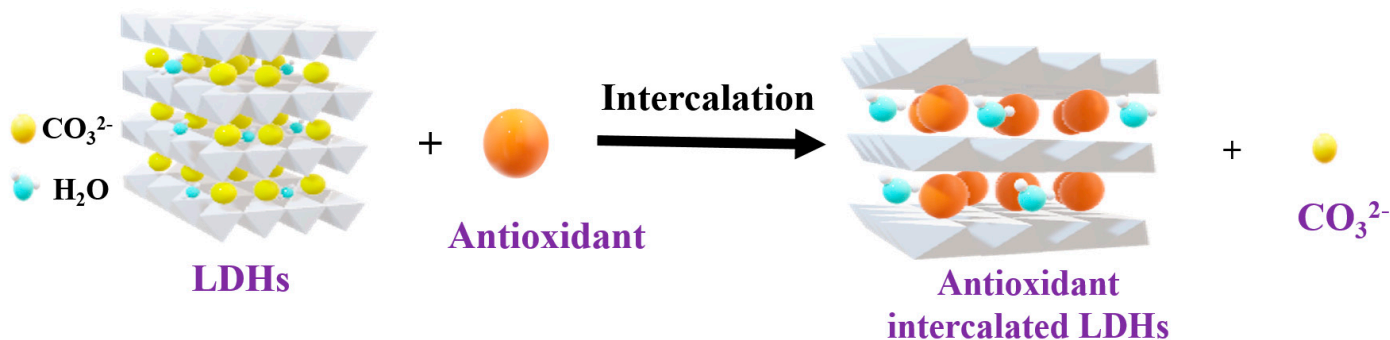


Figure 1. Schematic diagram of the synthesis of the LDHs antioxidants.

2.2.2. Characterizations of the Antioxidant Intercalated LDHs

The crystal structures of the LDHs and antioxidant intercalated LDHs were analyzed by an Empyrean XRD, manufactured by Malvern Panalytical, Alemlo, Netherlands. The X-ray source was Cu-K α radiation ($a = 0.15406$ nm), the scanning rate (2θ diffraction angle) was $10^\circ/\text{min}$, and the angle scanning range was $5^\circ\sim 70^\circ$. A Nicolet6700 FTIR (Thermo Fisher Scientific, Waltham, MA, USA) was used to characterize the chemical structure of LDHs intercalated with different antioxidants [32]. The wave number range was $400\sim 4000\text{ cm}^{-1}$, and the scan resolution was 2 cm^{-1} . A Zeiss Ultra plus SEM (Zeiss, Oberkochen, Germany) was used to examine the microscopic morphology of various antioxidant intercalated LDHs. A Lambda 750 s UV–Vis (Perkin-Elmer, Waltham, MA, USA) was used to measure the UV absorption and reflectance of LDHs intercalated with different antioxidants. The spectral wavelength was $200\sim 800\text{ nm}$, and the spectral resolution was 2 nm . The anti-aging abilities of different antioxidant intercalated LDHs were tested by the free radical capture test [34,35]. The basic idea is as below: The UV light is visibly absorbed by the purple DPPH ethanol solution, which has a peak wavelength of 517 nm . After the reaction of antioxidant intercalated LDHs with DPPH, the color of the solution became lighter, and the intensity of the absorption peak decreased. The ability of LDHs intercalated with antioxidants to capture free radicals can be identified by comparing the changes in UV absorbance at 517 nm of the DPPH ethanol solution. Formula (1) was used to calculate the free radical scavenging rate:

$$D(\%) = (A_0 - A_f)/A_0 \times 100\% \quad (1)$$

where A_0 is the absorbance of the DPPH ethanol solution, A_t is the absorbance of LDHs intercalated with antioxidants after a period of time, and D is the free radical scavenging rate.

2.3. Preparation and Characterizations of Antioxidant Intercalated LDHs-Modified Asphalt

2.3.1. Preparation of Antioxidant Intercalated LDHs-Modified Asphalt

Antioxidant intercalated LDHs-modified asphalt was prepared by the melt blending method. The asphalt was heated to 140 ± 5 °C, and the intercalated LDHs were gradually added by a high shear mixer at a 2000 r/min shear rate, and then, the shear rate was increased to 4000 r/min and sheared for 90 min [36]. The asphalts modified by LDHs, LDHs-1222, LDHs-TP, and LDHs-3 were denoted as LMB, LMB-1222, LMB-TP, and LMB-3, respectively.

2.3.2. Storage Stability Test

A storage stability test was conducted according to Chinese standard JTG E20-2011 [37], as 50 ± 5 g of modified asphalt was injected into a vertical 25 mm diameter aluminum tube, which was then fastened to a bracket and heated to 163 °C for 48 h. After cooling to 5 °C for 4 h, the tube was divided into three equal pieces. The softening points of the upper and lower ends were measured. The smaller the difference of the softening points between the two ends, the better the compatibility between the modifier and asphalt.

2.3.3. Thin Film Oven Test (TFOT)

Using a thin film oven, the modified asphalts underwent short-term thermal oxidation aging based on Chinese standard JTG E20-2011, as 50 ± 5 g of melted asphalt was poured into the aging plate and aged at 163 °C for 5 h.

2.3.4. UV Aging Test

For the aging test, 20 g of the asphalt after TFOT aging was poured into an aging tray and then put into a UV aging chamber, and the intensity of the UV radiation was set at 20 W/m². The aging temperature was 50 ± 0.5 °C, and the UV aging was carried out for 7 days [38].

2.3.5. Physical Property Tests

The penetration (25 °C), softening point, ductility (10 °C), and viscosity (135 °C) of the modified asphalts before and after aging were tested according to Chinese standard JTG E20-2011. According to the degrees of change of the physical properties of asphalts before and after aging, the anti-aging abilities of different asphalts were evaluated. The evaluation parameters were the residual penetration ratio (RPR), softening point increment (SPI), ductility retention rate (DRR), and viscosity aging index (VAI). The RPR, SPI, DRR, and VAI were calculated according to the Formulas (2)–(5), respectively.

$$\text{RPR (\%)} = (P_2/P_1) \times 100\% \quad (2)$$

$$\text{SPI (°C)} = (SP_2 - SP_1) \quad (3)$$

$$\text{DRR (\%)} = (D_2/D_1) \times 100\% \quad (4)$$

$$\text{VAI (\%)} = (V_2 - V_1)/V_1 \times 100\% \quad (5)$$

where the P, SP, D, and V represent the penetration, softening point, ductility, and viscosity of the asphalt samples, respectively. The subscripts '1' and '2' represent the measured values of the asphalt samples before and after aging, respectively.

2.3.6. Rheological Property Test

Using a dynamic shear rheometer (DSR), the rheological characteristics of the various modified asphalts were evaluated both before and after aging by referring to Chinese standard JTG E20-2011. The temperature scanning range was 30 °C~80 °C, the scanning frequency was 10 rad/s, and the heating rate was 2 °C/min.

2.3.7. FTIR Test

The changes in the functional groups of the modified asphalts after aging were analyzed using the FTIR test [39,40]. A thin film was created by dissolving 10 mg of bitumen in 2 mL of CS₂, which was then deposited onto a KBr electrolyzer and dried. The test was carried out in the wavenumber range of 400 cm⁻¹ to 4000 cm⁻¹, and the test scanning resolution was 2 cm⁻¹. The aging degrees of the asphalts were quantitatively analyzed by Formulas (6)–(8).

$$I_{C=O} = A_{1700} / \Sigma A \quad (6)$$

$$I_{S=O} = A_{1030} / \Sigma A \quad (7)$$

$$\Sigma A = A_{3780} + A_{3690} + A_{2927} + A_{2856} + A_{2721} + A_{2354} + A_{1700} + A_{1593} + A_{1455} + A_{1375} + A_{1030} + A_{864} + A_{813} + A_{740} \quad (8)$$

where the $I_{C=O}$, $I_{S=O}$, and A_X are the carbonyl aging index, sulfoxide aging index, and characteristic peak area, respectively.

3. Results and Discussion

3.1. Characterization of the Antioxidant Intercalated LDHs

3.1.1. Crystal Structure Analysis

Figure 2 displays the XRD patterns of unintercalated LDHs and LDHs intercalated with various antioxidants. The graphic demonstrates that they all have robust and distinct diffraction peaks, indicating that they all have a regular crystal structure and layered structure. After the intercalation of several antioxidants, the d_{003} diffraction peak of the LDHs moved from 11.64° to lower angles, the d_{003} diffraction peak of LDHs-3 moved to 4.06°, the d_{003} diffraction peak of LDHs-TP moved to 6.00°, and the d_{003} diffraction peak of LDHs-1222 moved to 5.13°. This indicated that several antioxidant molecules were successfully inserted into the interlayer of LDHs, replacing the original CO₃²⁻ in the interlayer.

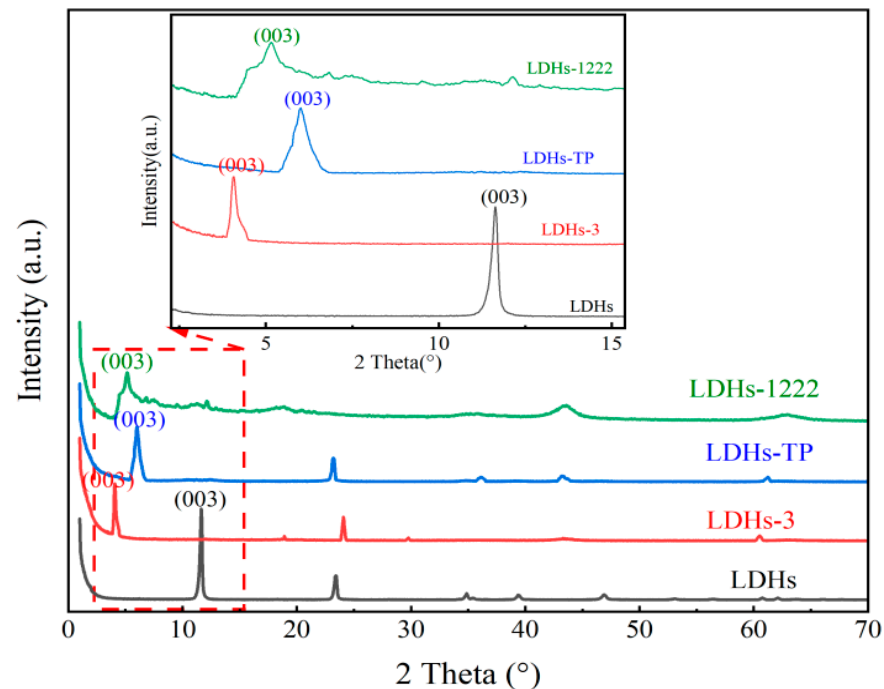


Figure 2. XRD patterns of the LDHs and different antioxidant intercalated LDHs.

According to the peak position of the d_{003} diffraction peak in the spectrum, the Bragg equation, presented in Formula (9), can be used to determine the interlayer spacing of the LDHs.

$$2d\sin\theta = n\lambda \quad (9)$$

where λ is the wavelength of the X-ray incident wave, and the X-ray source used in this test is Cu-K α radiation, $\lambda = 0.15406$ nm; n is the diffraction order, as, for the d_{003} diffraction peak, $n = 1$; and θ is the diffraction angle. It can be calculated that the interlayer distance of the LDHs is 0.76 nm, the interlayer distance of LDHs-3 is 2.17 nm, the interlayer distance of LDHs-TP is 1.47 nm, and the interlayer distance of LDHs-1222 is 1.72 nm. The increases in the interlayer distance of the LDHs indicated that antioxidants entered the interlayer of LDHs and different antioxidants intercalated LDHs were prepared successfully.

3.1.2. FTIR Analysis

The FTIR spectra of the LDHs and LDHs intercalated with different antioxidants are shown in Figure 3. For the spectrum of LDHs, a very strong and wide absorption peak appeared at 3452 cm^{-1} , which was formed by the stretching vibration of water molecules between the layers of the LDHs. A wide shoulder peak appeared near 3071 cm^{-1} , which was formed by the interaction between the hydroxyl group and interlayer CO_3^{2-} . A sharp absorption peak appeared at 1360 cm^{-1} , which was formed by the antisymmetric stretching vibration absorption peak of interlayer CO_3^{2-} . The peak did not undergo any splitting, indicating that CO_3^{2-} was in a very symmetrical position between the layers of the LDHs. After the intercalation of the antioxidants, the absorption peaks of the LDHs changed greatly. The absorption peak of CO_3^{2-} in the interlayer of the LDHs disappeared at 1360 cm^{-1} , indicating that the CO_3^{2-} in the interlayer of the LDHs was completely replaced by antioxidants, which was consistent with the disappearance of the diffraction peak at 11.64° in the XRD spectrum (Figure 2). Moreover, the characteristic absorption peaks of antioxidant molecules could still be observed in the intercalated LDHs. The carboxyl characteristic peaks of antioxidant 3, the phosphorus–oxygen bond characteristic peaks of antioxidant 1222, and the carbon–sulfur bond characteristic peaks of antioxidant TP were observed at 1700 cm^{-1} , 1060 cm^{-1} , and 960 cm^{-1} , respectively. This indicated that the antioxidants did not decompose after the intercalation.

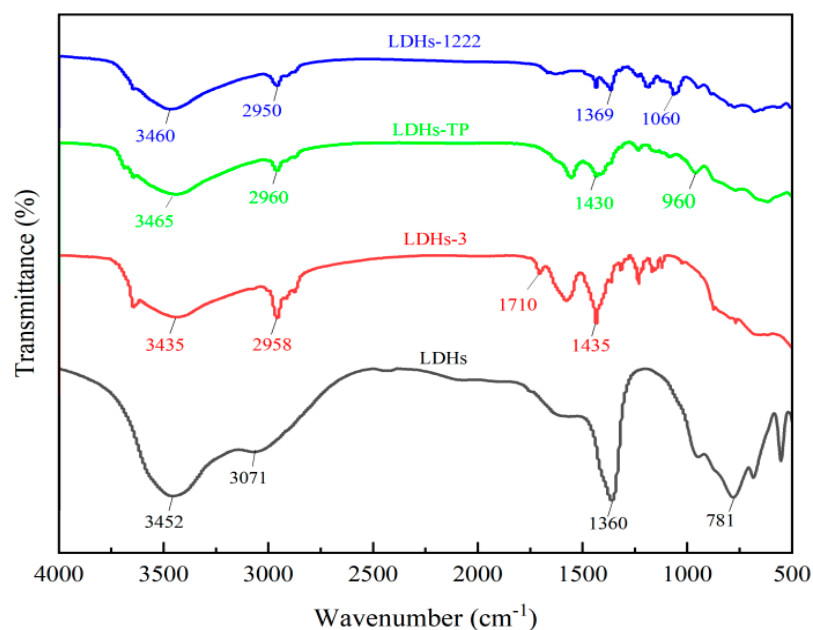


Figure 3. FTIR spectra of the LDHs and antioxidant intercalated LDHs.

3.1.3. Micromorphology Analysis

The micromorphology of the LDHs and LDHs intercalated with different antioxidants are shown in Figures 4 and 5.

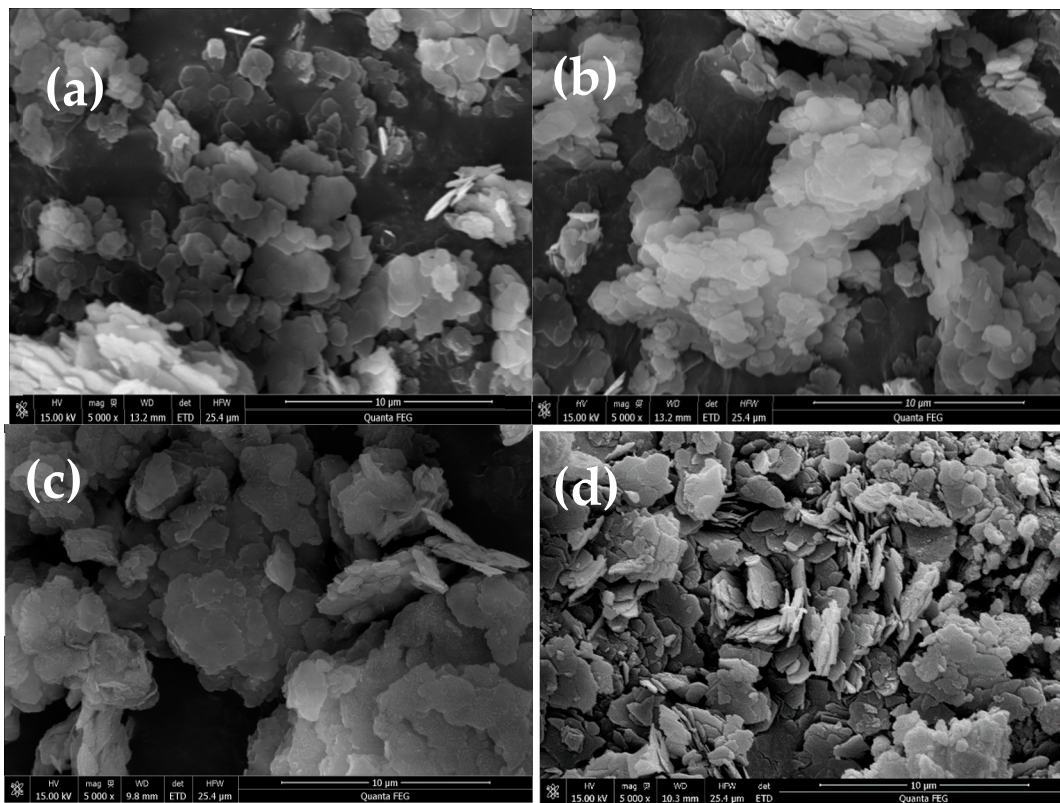


Figure 4. Micromorphology of the LDHs and different antioxidant intercalated LDHs ($\times 5000$): (a) LDHs, (b) LDHs-3, (c) LDHs-TP, and (d) LDHs-1222.

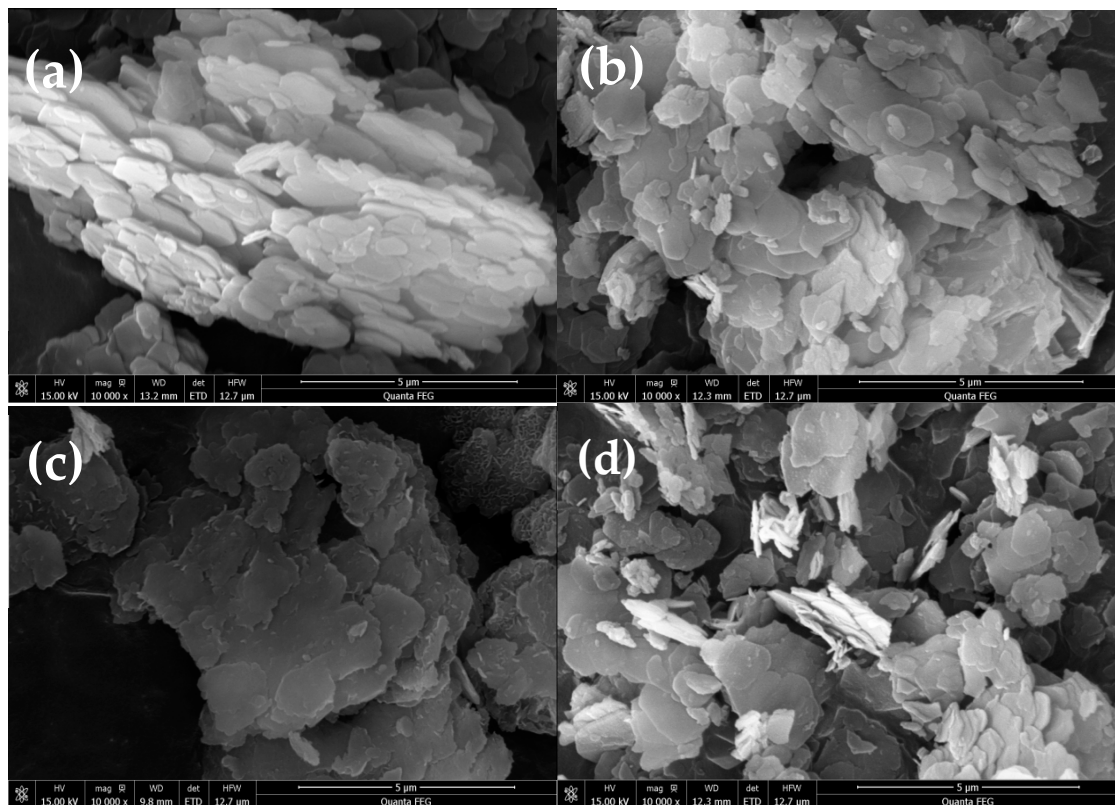


Figure 5. Micromorphology of the LDHs and different antioxidant intercalated LDHs ($\times 10,000$): (a) LDHs, (b) LDHs-3, (c) LDHs-TP, and (d) LDHs-1222.

From Figure 4a, it can be seen that LDHs have nonuniform lamellar structures, and their particle size varies greatly in the 0.9 μm –2 μm range. The LDHs after antioxidant intercalation (Figure 5b–d) still maintained their lamellar structure, and the number of particles with small particle sizes decreased. It can be seen from Figure 5 that the particle size of the LDHs after intercalation is more uniform, and the surface becomes rough. This is due to the secondary growth of LDHs molecules during the intercalation of the antioxidant molecules, which makes LDHs with small particle sizes grow again. The particle size range is about 1.2 μm –2 μm . In addition, the antioxidant molecules increase the interlayer spacing of LDHs and thus increase its thickness.

3.1.4. UV–Vis Spectroscopy Analysis

The absorption spectra of the LDHs and LDHs intercalated with various antioxidants to UV–Visible light in the 200–800 nm range are shown in Figure 6. It can be seen from the figure that LDHs have a certain absorption capacity for UV light in the range of 200–300 nm and have almost no absorption capacity in other bands. In contrast, the UV absorption capacity of the antioxidant intercalated LDHs in the range of 200–400 nm was greatly increased, and the order of the UV absorption ability from strong to weak was LDHs-TP > LDHs-3 > LDHs-1222 > LDHs. The three kinds of antioxidant intercalated LDHs have the strongest absorption peak near 300 nm, and the UV light in this band has the greatest damage to asphalt [41], indicating that the intercalated LDHs can effectively protect asphalt from UV damage. This is because antioxidant 3 contains a benzene ring and carboxyl group, antioxidant TP contains a carbon–sulfur double bond, and these functional groups can absorb the energy of UV light.

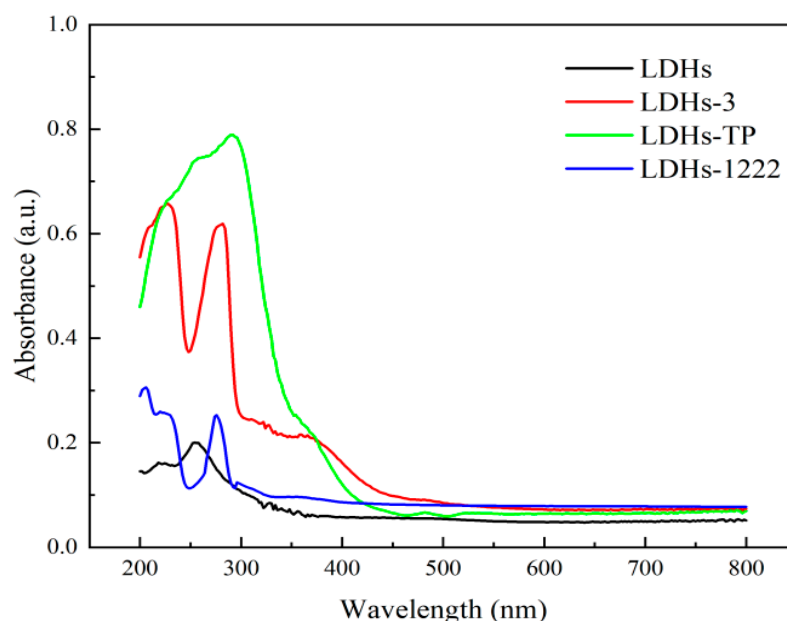


Figure 6. UV–Vis absorption spectra of the LDHs and different antioxidants intercalated LDHs.

The UV–Visible reflectance spectra of the LDHs and different antioxidants intercalated LDHs are shown in Figure 7. The intercalation of several antioxidants reduced the reflectivity of the LDHs. Compared to Figure 6, it was found that, in the range of 200–400 nm, the stronger the ultraviolet absorption capacity, the weaker the reflection ability of the modifier. This also showed that the interlayer antioxidant had a strong ultraviolet absorption capacity, because in the case of a certain incident light, the more ultraviolet light absorbed by the modifier, the less ultraviolet light was reflected.

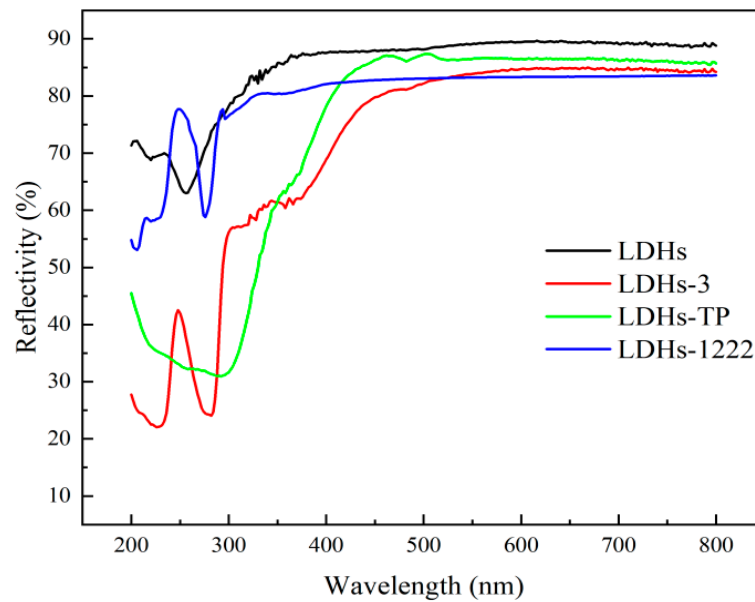


Figure 7. UV-Vis reflectance spectra of the LDHs and different antioxidants intercalated LDHs.

3.1.5. Free Radical Scavenging Performance Analysis

Figure 8 shows the free radical scavenging UV spectra of the LDHs and LDHs intercalated with different antioxidants after 2 h of reaction with DPPH. From the diagram, it can be known that, after adding the LDHs, the absorbance of the DPPH solution decreased. The reason is that the free radical solution has high activity and is easily affected by external temperature, light, oxygen, and other conditions. After calibration according to the baseline, the absorbance of DPPH, LDH-TP, LDHs-1222, and LDHs-3 at 517 nm were 0.416, 0.345, 0.268, and 0.176, respectively. According to Formula (1), the corresponding free radical scavenging rates were 17.1%, 35.6%, and 57.7%, respectively. Therefore, the free radical scavenging ability of LDHs-3 is the best, the ability of LDHs-1222 is in the middle, and the ability of LDHs-TP is the worst.

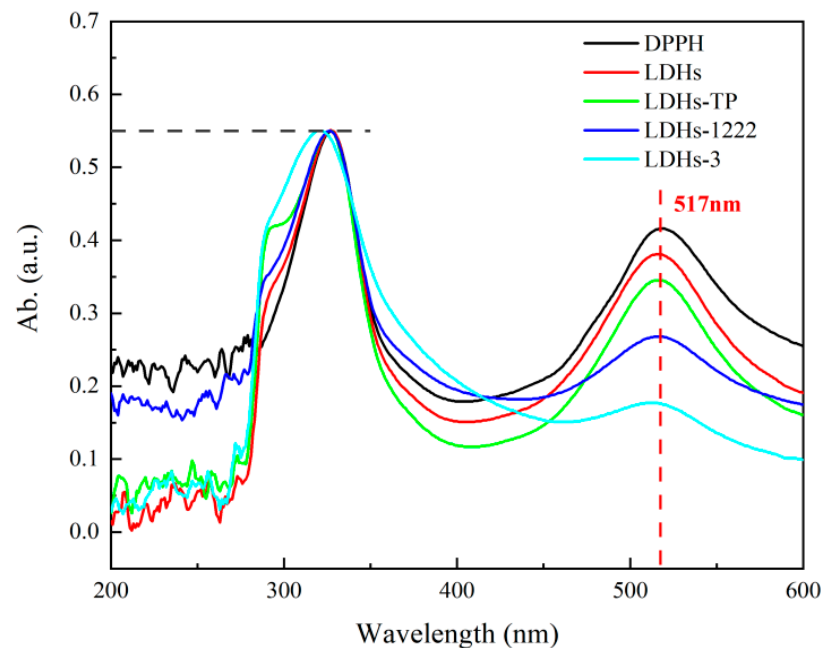


Figure 8. UV-Vis spectra of the DPPH solutions with and without the modifiers.

Figure 9 shows the free radical scavenging UV–Vis spectra of the DPPH solution with LDHs-3 at different reaction times. It can be seen from the figure that the absorbance at 517 nm after 0.5 h, 1 h, 1.5 h, and 2 h of the reaction was 0.354, 0.312, 0.206, and 0.176, respectively. The free radical scavenging rates corresponding to different reaction times were 14.9%, 25%, 50.5%, and 57.7%, respectively. As a result, the antioxidant intercalated LDHs' ability to scavenge free radicals improved with longer reaction times. The results proved that the three antioxidants' intercalation increased the ability of LDHs to scavenge free radicals, and LDHs-3 had the best free radical scavenging ability.

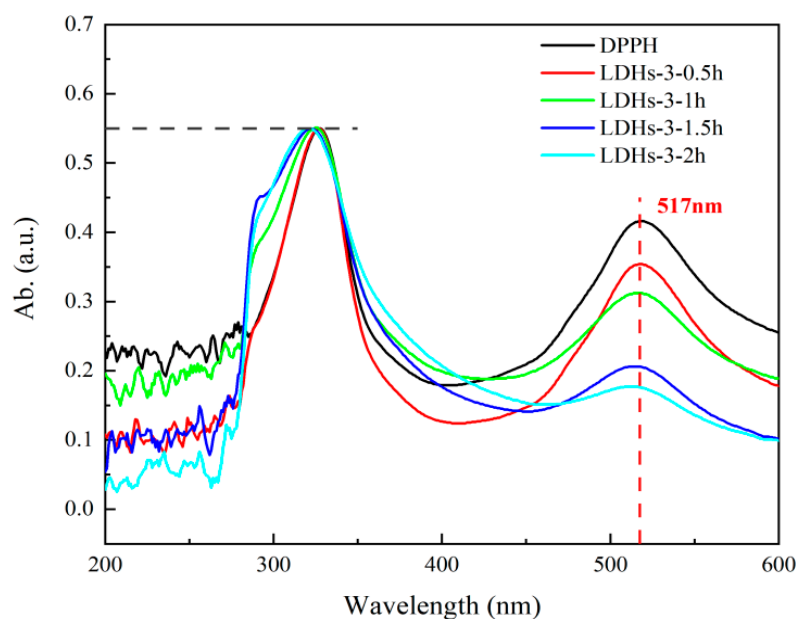


Figure 9. UV–Vis spectra of the DPPH solution with LDHs-3 at different reaction times.

3.2. Effects of Antioxidant Intercalated LDHs on Asphalt Performance

3.2.1. Physical Properties

Table 2 shows the physical properties of the base asphalt and the asphalts blended with different LDHs modifiers. The table shows that the physical properties of the modified asphalts vary according to the same pattern. As the modifier content increases, the penetration and ductility of the modified asphalt decrease, while the softening point and viscosity increase. This is because these several modifiers have lamellar structures, which will hinder the movement of asphalt molecules and increase the consistency of asphalt after being incorporated into the asphalt. The addition of LDHs will greatly decrease the ductility of asphalt. The reason for this is the poor compatibility between LDHs and asphalt. LDHs are prone to agglomeration, and the modified asphalt is prone to stress concentration. LDHs and asphalt have increased compatibility after antioxidant intercalation, allowing the LDHs modifier to be distributed more evenly throughout the asphalt and improving the modified asphalts' ductility. The penetration of 6% LMB decreased by 6.7 dmm compared to that of the base asphalt, while that of LMB-3, LMB-1222, and LMB-TP decreased by 3.6 dmm, 4.1 dmm, and 4.5 dmm, respectively. The softening point and viscosity of the modified asphalts were increased, because the modifiers increased the consistency and internal friction of asphalt. In a word, the effect of antioxidant intercalation LDHs on the physical properties of asphalt was less than that of the LDHs.

Table 2. Effects of different modifiers on the physical properties of asphalt.

Asphalt Type	Penetration (25 °C, dmm)	Softening Point (°C)	Ductility (10 °C, cm)	Viscosity (135 °C, Pa.S)
Base asphalt	72.7	48.3	19.2	0.4725
2%LMB	70.2	49.5	17.5	0.5103
4%LMB	68.5	51.2	14.2	0.5355
6%LMB	66.0	52.	11.7	0.5870
2%LMB-TP	70.5	49.3	18.2	0.5913
4%LMB-TP	69.1	51.2	16.5	0.5988
6%LMB-TP	68.2	51.8	15.8	0.6188
2%LMB-1222	71.8	48.9	18.1	0.4794
4%LMB-1222	70.3	49.6	16.6	0.4939
6%LMB-1222	68.6	51.1	15.5	0.5015
2%LMB-3	71.5	50.3	18.4	0.5867
4%LMB-3	70.8	51.2	17.4	0.5935
6%LMB-3	69.1	52.5	15.8	0.6271

3.2.2. Rheological Properties

Figure 10 shows the effect of the modifiers with different contents on the complex modulus (G^*) of asphalt. G^* reflects the resistance of the asphalt to deformation under external forces, and a higher G^* value denotes a greater resistance of the asphalt to deformation. It can be seen from Figure 10 that, with the increase in the modifier content, the G^* of LMB increases gradually. When the content in the LDHs modifier increases from 2% to 4%, the G^* of the modified asphalt increases greatly, while the increase in G^* decreases obviously as the content of the LDHs modifier increases from 4% to 6%. The rationale is that, by adding LDHs, the stiff component in asphalt is increased, which improves the asphalt's ability to withstand deformation. As the content continues to increase, LDHs particles agglomerate in the asphalt, and their modification effect decreases. Compared to LDHs, the addition of LDHs-3 increases the G^* of the asphalt to a lower extent due to its good compatibility with asphalt. With an increase in the LDHs-3 dose, the G^* of LMB-3 rises. Compared to the dosage of 4%, the dosage of 6% does not significantly increase the G^* of asphalt, which is probably due to the fact that the high dosage of LDHs-3 leads to segregation. Therefore, 4% is an appropriate dosage of the LDHs modifiers, which is consistent with the findings of Chen et al. [28].

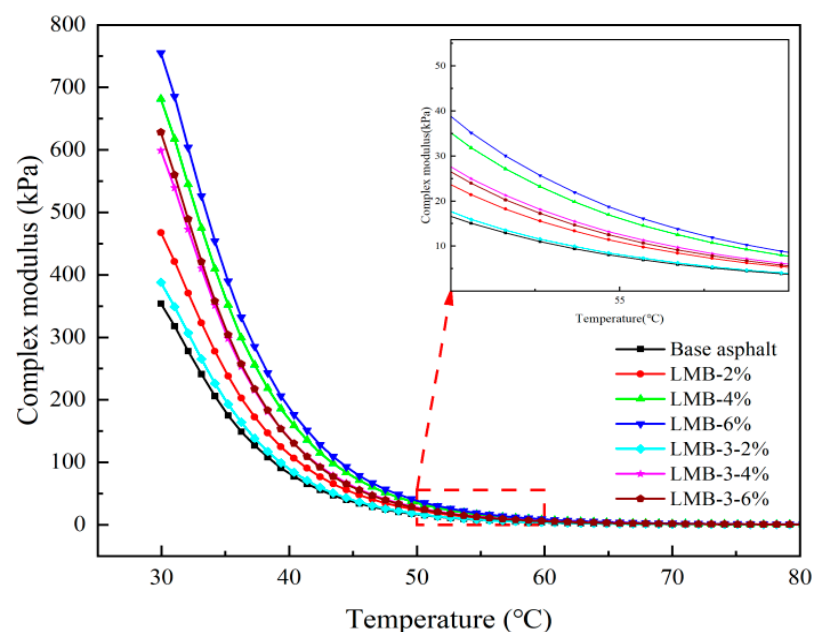
**Figure 10.** Effects of different contents of the modifier on the complex modulus of asphalt.

Figure 11 shows the influence of different modifiers on the complex modulus (G^*) and phase angle (δ) of asphalt under the same dosage of 4%. It can be seen from Figure 11 that, when the LDHs modifiers concentration is 4%, these several modifiers increase the G^* of asphalt and decrease its δ . By increasing the internal friction of the asphalt flow, LDHs improve the asphalt's resistance to deformation as compared to the base asphalt. The additions of LDHs-3, LDHs-1222, and LDHs-TP also have the same effect. Due to their better compatibility with asphalt, they are more evenly dispersed in asphalt, resulting in a lower G^* and higher δ than LMB.

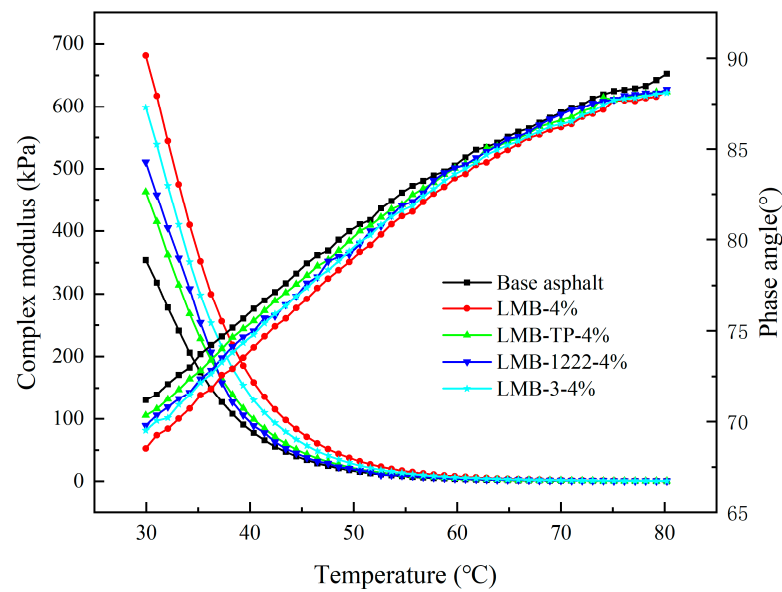


Figure 11. Effects of different modifiers on the rheological properties of asphalt.

3.2.3. Storage Stability

Table 3 displays the storage stability of different modified asphalts. The smaller the ΔS , the better the compatibility between asphalt and the modifier. The table shows that the ΔS of various modified asphalts rise as the modifier concentration is increased. The ΔS of LMB are the largest. When the content of the LDHs is 6%, the ΔS is 2.1 °C. This indicates that the LDHs particles agglomerate in the asphalt and settle at the bottom of the test tube. In contrast, ΔS can be effectively reduced after antioxidant intercalation. The ΔS of LMB-3, LMB-1222, and LMB-TP with the 6% content of the modifiers decreased to 0.4 °C, 0.6 °C, and 0.7 °C, respectively. This meant that the intercalation of antioxidant significantly improved the compatibility of the LDHs and asphalt. Specifically, LMB-3 had the highest storage stability.

Table 3. Effects of different modifiers on the storage stability of asphalt.

Asphalt Type	Upper Softening Point (°C)	Lower Softening Point (°C)	ΔS (°C)
2%LMB	49.6	50.5	0.9
4%LMB	51.3	52.8	1.5
6%LMB	52.5	54.6	2.1
2%LMB-TP	49.5	49.9	0.4
4%LMB-TP	51.4	52.1	0.5
6%LMB-TP	52.1	53	0.7
2%LMB-1222	49.0	49.3	0.3
4%LMB-1222	49.8	50.2	0.4
6%LMB-1222	51.6	52.2	0.6
2%LMB-3	50.5	50.7	0.2
4%LMB-3	51.4	51.7	0.3
6%LMB-3	52.7	53.1	0.4

3.3. Effect of Antioxidant Intercalated LDHs on the Anti-Aging Properties of Asphalt

3.3.1. Physical Properties of Different Modified Asphalts after Aging

Figures 12–15 reflect the RPR, SPI, DRR, and VAI of different modified asphalts after TFOT aging and UV aging, respectively, and the content of each modifier is 4%. The higher the RPR and DRR and the lower the SPI and VAI, the stronger the anti-aging effectiveness of the modified asphalt. The physical properties of several types of asphalt were decreased after TFOT aging. The RPR, SPI, DRR, and VAI of the base asphalt were 75.1%, 3.1 °C, 45.3%, and 25.7%, respectively. The LDHs modifiers enhance the asphalt's anti-aging capability, and the anti-thermal oxidation aging capabilities of the modified asphalts are in the following order: LMB-1222 > LMB-3 > LMB-TP > LMB > base asphalt. The light components in asphalt will volatilize at high temperatures, and oxygen will permeate the asphalt to react with the active functional groups. These several LDHs modifiers are in lamellar structures, which can inhibit the volatilization of light components and the penetration of oxygen. The LDHs intercalated by antioxidants exhibit greater asphalt compatibility and inhibitory action. The thermal oxidation aging of asphalt is a free radical chain reaction process [42]. Antioxidants can capture free radicals and thus enhance the thermal oxidation aging resistance of asphalt [43]. Therefore, these several antioxidant intercalated LDHs modifiers further enhanced the thermal oxygen oxidation resistance of asphalt. In contrast, LMB-1222 has the best thermal oxidation aging resistance.

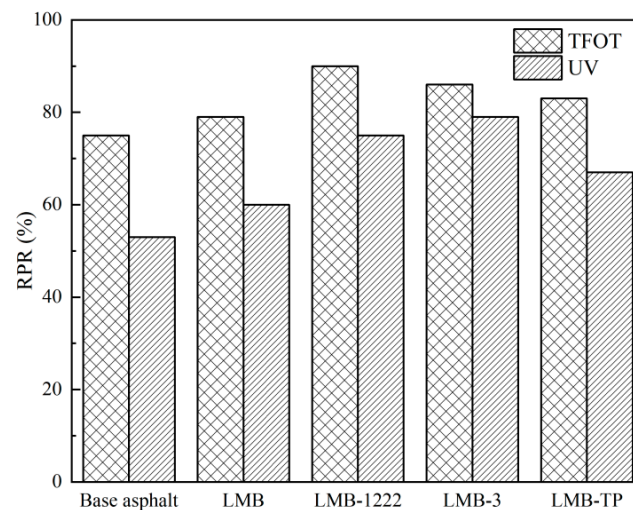


Figure 12. RPR of different modified asphalts after TFOT aging and UV aging.

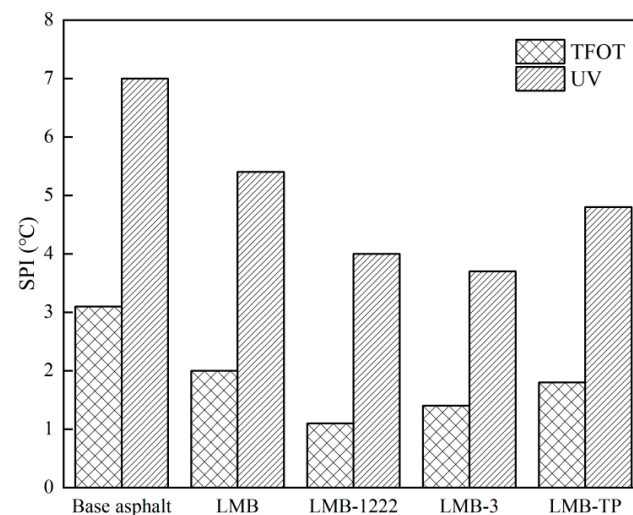


Figure 13. SPI of different modified asphalts after TFOT aging and UV aging.

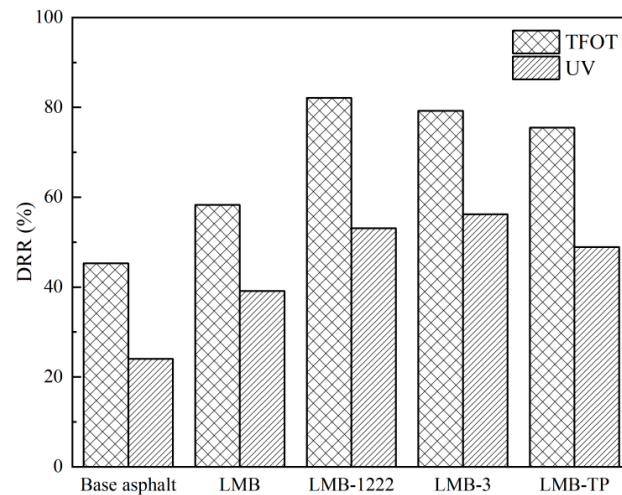


Figure 14. DRR of different modified asphalts after TFOT aging and UV aging.

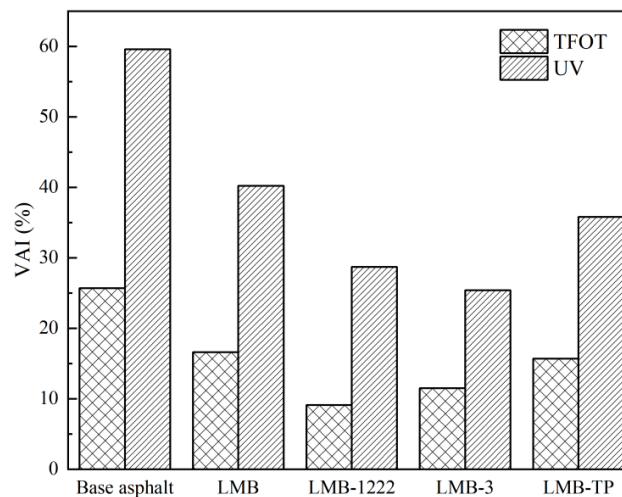


Figure 15. VAI of different modified asphalts after TFOT aging and UV aging.

After UV aging, the aging degrees of the asphalts are significantly higher than those after TFOT aging. The RPR, SPI, DRR, and VAI of the base asphalt were 53.3%, 7 °C, 24.0%, and 59.6%, respectively. After adding several LDHs modifiers, the aging degrees of the asphalts were reduced. The aging resistances of the different asphalts are in the order of LMB-3 > LMB-1222 > LMB-TP > LMB > base asphalt. UV rays have high energy, which will break some chemical bonds in asphalt and promote asphalt aging. The lamellar structure of LDHs can reflect UV light, and after intercalation, the antioxidant molecules between the layers can absorb UV light [28]. In addition, asphalt will also produce free radicals during UV aging, which can also be captured by antioxidant molecules between the interlayers of LDHs. Therefore, these several antioxidant intercalated LDHs modifiers can enhance the UV aging resistance of asphalt. In contrast, LMB-3 has the best anti-UV aging effect. This is because LDHs-3 has both good UV absorption and UV reflectivity. The results of this research are consistent with the results obtained in the literature. Antioxidant intercalated LDHs have both the functions of LDHs and antioxidants and can simultaneously enhance the thermal oxidation and ultraviolet aging resistances of asphalt.

3.3.2. Rheological Properties of Different Modified Asphalts after Aging

After TFOT aging and UV aging, the complex modulus of asphalt underwent quantitative analysis. Formulas (10) and (11) were used to calculate the ratio of the complex modulus (GAI) after TFOT and UV aging to the complex modulus before aging.

$$\text{GAI}_{(\text{TFOT})} = G_{\text{TFOT}}/G_0 \quad (10)$$

$$\text{GAI}_{(\text{UV})} = G_{\text{UV}}/G_0 \quad (11)$$

In the formulas, the complex modulus of asphalt prior to aging, after TFOT aging, and after UV aging are designated as G_0 , G_{TFOT} , and G_{UV} , respectively.

The GAI curves of modified asphalt after TFOT aging with different contents of LDHs-TP are drawn in Figure 16 to explore the optimum dosage of the modifier for asphalt anti-aging. The diagram demonstrates that the GAI values of base asphalt are at their maximums during thermal oxidation aging. It shows that the aging of the base asphalt is the most serious. The addition of LDHs-TP reduces the GAI, indicating that it delays the TFOT aging of asphalt. With the increase in the LDHs-TP content, GAI decreases first and then increases. When the dosage is 4%, the modified asphalt has the best resistance to thermal oxidation aging. This is because excessive LDHs modifier will lead to segregation. Therefore, 4% of the LDHs modifier has good compatibility with asphalt and can significantly increase the anti-aging performance of asphalt.

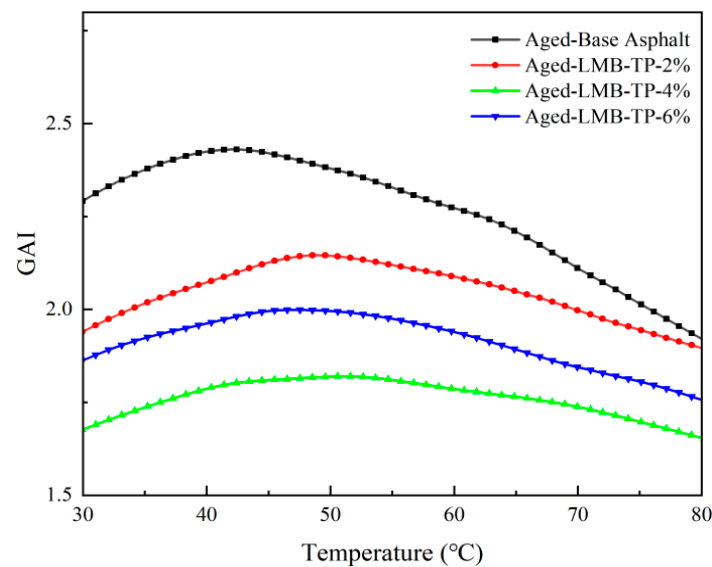


Figure 16. GAI of the modified asphalts after TFOT aging with different contents of LDHs-TP.

Figure 17 shows the GAI curves of the base asphalt and modified asphalts with different contents of LDHs-TP after UV aging. The diagram shows that, after UV aging, the asphalts' GAI considerably increases, indicating that the aging degrees of the asphalts are further deepened. In contrast, the asphalts' ability to resist UV aging is greatest when the modifier content is 4%, which is consistent with the result of previous research [32].

Figure 18 shows the GAI curves of different anti-aging agents' modified asphalts after TFOT aging. Compared to the base asphalt, the additions of these various LDHs modifiers significantly lower the GAI of asphalt after TFOT aging and enhance the asphalt's anti-aging property. The GAI of the asphalts are in the order of base asphalt > LMB-4% > LMB-TP-4% > LMB-3-4% > LMB-1222-4%. The LDHs after antioxidant intercalation have better anti-aging effects; among which, LMB-1222 has the best resistance to thermal oxidation aging.

Figure 19 shows the GAI curves of different LDHs modified asphalts after UV aging. The asphalts' GAI after UV aging is higher than the GAI after TFOT aging, suggesting that the asphalts have been aged more severely. The order of the GAI after UV aging is base asphalt > LMB-4% > LMB-TP-4% > LMB-1222-4% > LMB-3-4%. It can be seen from the previous experiments that LDHs-3 has both a good UV absorption rate and reflectivity, which shows that LMB-3 have the best anti-UV aging effect.

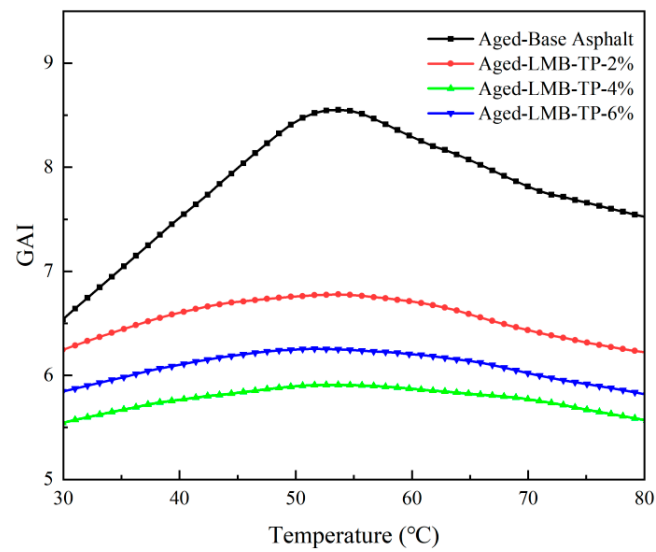


Figure 17. GAI of the modified asphalts with different dosages of LDHs-TP after UV aging.

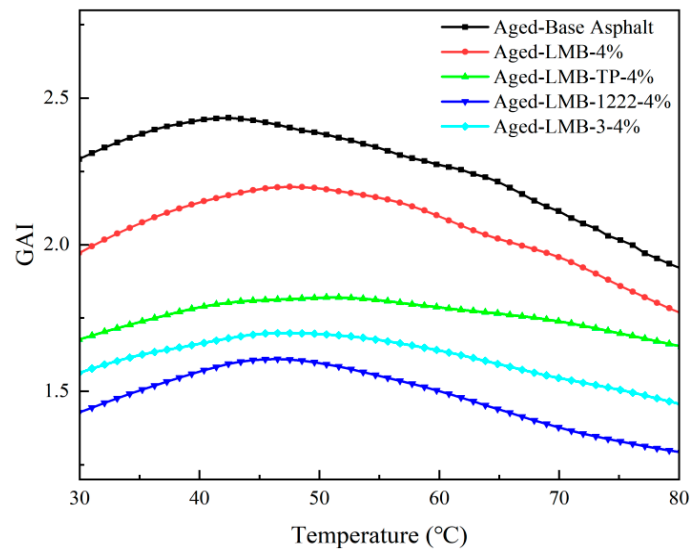


Figure 18. GAI of the different modified asphalts after TFOT aging.

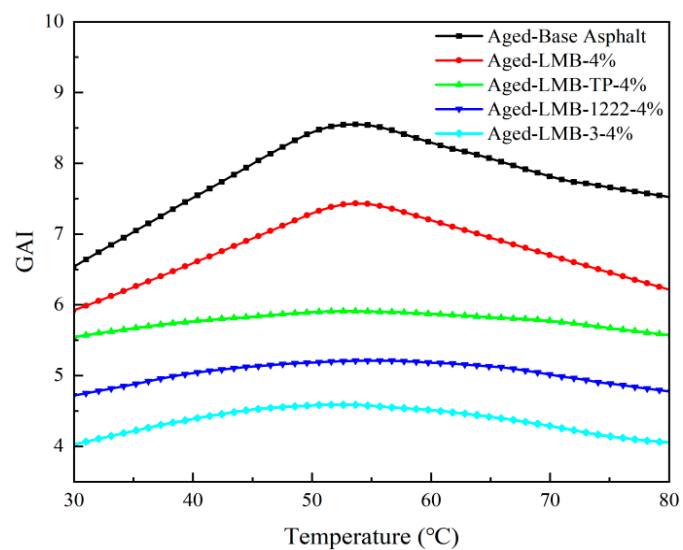


Figure 19. GAI of the different modified asphalts after UV aging.

3.3.3. Changes in Functional Groups of Different Modified Asphalts after Aging

Figure 20 shows the FTIR diagrams of various asphalts before aging, and Figures 21 and 22 are the FTIR diagrams of various asphalts after TFOT aging and UV aging, respectively. The peak corresponding functional group at 1700 cm^{-1} is carbonyl (C=O), and the peak corresponding functional group at 1030 cm^{-1} is sulfoxide (S=O). After the earlier experiments, it can be known that, when the dosage of the LDHs modifiers is 4%, the modified asphalts have the best anti-aging qualities, so the dosage of the modifiers used in the FTIR test is 4%. It can be seen from Figures 20–22 that there are almost no absorption peaks at 1700 cm^{-1} and 1030 cm^{-1} when the asphalts are not aged. After TFOT aging, these modified asphalts have a weak absorption peak at 1030 cm^{-1} . After UV aging, the absorption peak of each asphalt at 1030 cm^{-1} is obviously strengthened, and the absorption peak can also be observed at 1700 cm^{-1} . This shows that the aging degree of asphalt after UV aging is deepened. The increment of the sulfoxide group after asphalt aging is larger than that of the carbonyl group. This is owed to the asphalt's active chemical properties, which cause sulfur-containing functional groups to oxidize more quickly.

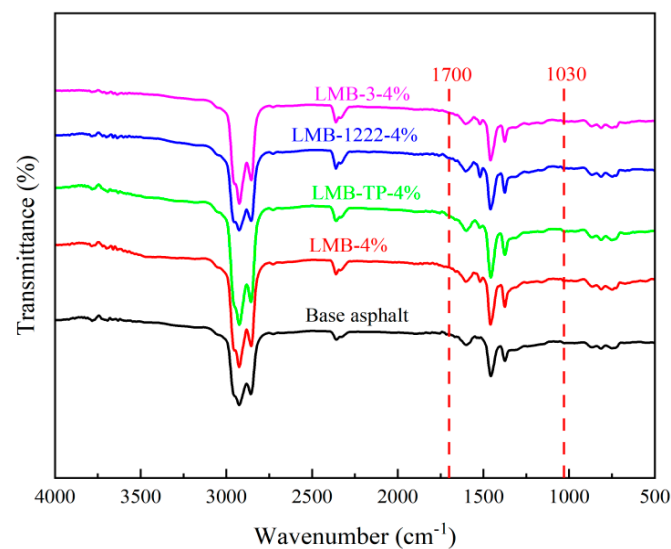


Figure 20. FTIR spectra of the base asphalt and different modified asphalts before aging.

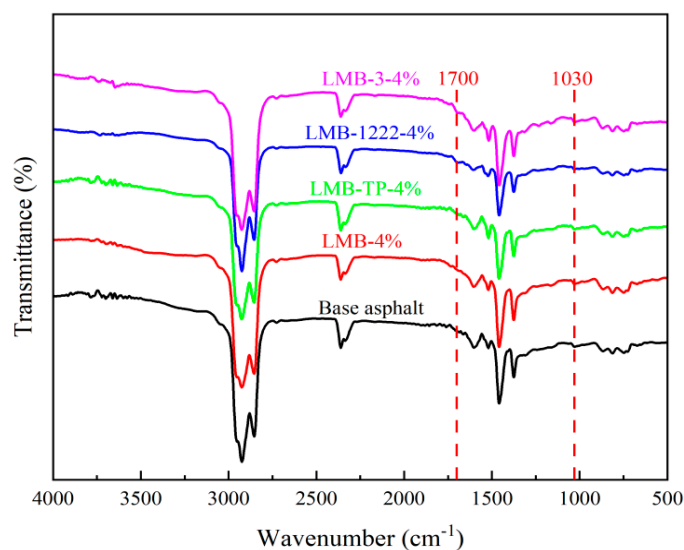


Figure 21. FTIR spectra of the different modified asphalts after TFOT aging.

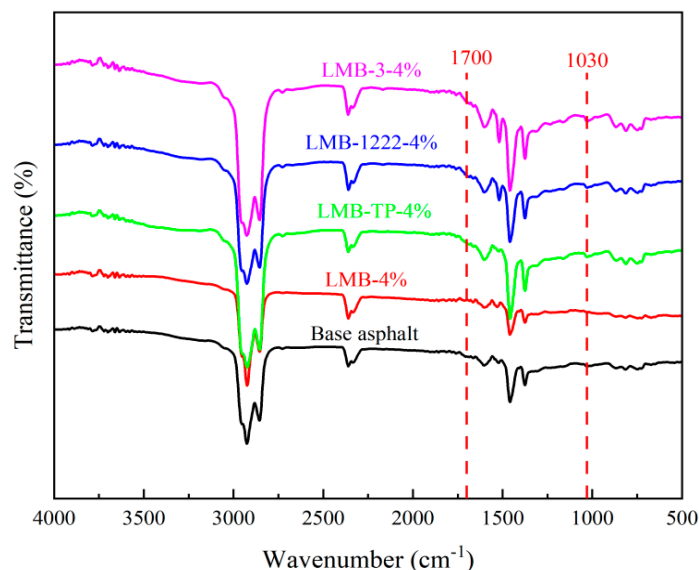


Figure 22. FTIR spectra of the different modified asphalts after UV aging.

Table 4 shows the carbonyl and sulfoxide aging indices of the base asphalt and different modified asphalts before and after aging. Before aging, LMB-3 has the highest carbonyl content, and LMB-1222 has the highest sulfoxide content. The reason is that the antioxidant 3 molecule contains a carbonyl group, and the antioxidant 1222 molecule contains a P-O bond. The peak of the P-O bond is very close to the peak of the sulfoxide group, and the overlap between the two peaks makes the $I_{S=O}$ value larger. After TFOT aging, the asphalts' $I_{C=O}$ and $I_{S=O}$ values increased, with the base asphalt's $I_{C=O}$ and $I_{S=O}$ increments being 1.63 and 8.6, respectively. After adding the LDHs modifiers, the increments of $I_{C=O}$ and $I_{S=O}$ of the asphalt decreased, indicating that these LDHs modifiers inhibited the aging of asphalt. Among them, LMB-1222 has the best thermal oxidation aging resistance. The increments of $I_{C=O}$ and $I_{S=O}$ of these asphalts increased more during UV aging, indicating that the asphalts were subjected to more serious aging. The base asphalt's $I_{C=O}$ and $I_{S=O}$ values were 17.63 and 22.9, respectively. Different LDHs-modified asphalts have better anti-UV aging effects. LMB-3 shows a minimal $\Delta I_{C=O}$ and $\Delta I_{S=O}$ of 7.58 and 11.75, respectively, indicating that LMB-3 has the best anti-UV effect.

Table 4. Aging indices of the base asphalt and different modified asphalts before and after aging.

Asphalt Types	Aging Index ($\times 10^{-3}$)									
	Unaged		TFOT Aged				UV Aged			
	$I_{C=O}$	$I_{S=O}$	$I_{C=O}$	$\Delta I_{C=O}$	$I_{S=O}$	$\Delta I_{S=O}$	$I_{C=O}$	$\Delta I_{C=O}$	$I_{S=O}$	$\Delta I_{S=O}$
Base asphalt	0.98	9.48	2.61	1.63	18.08	8.60	18.61	17.63	32.38	22.90
LMB-4%	1.01	9.83	2.24	1.23	15.54	5.71	12.27	11.26	28.74	18.91
LMB-TP-4%	1.05	11.15	1.96	0.91	16.36	5.21	9.25	8.20	26.48	15.33
LMB-1222-4%	1.03	14.84	1.87	0.84	18.21	4.37	9.08	8.05	30.65	15.81
LMB-3-4%	2.16	10.82	2.43	0.87	15.89	5.07	9.74	7.58	22.57	11.75

4. Conclusions

In this paper, three antioxidants (antioxidant 3, antioxidant 1222, and antioxidant TP) were inserted into the interlayer of LDHs by the ion exchange method to prepare different antioxidant intercalated LDHs, and then, they were blended into asphalt to enhance its anti-aging property. By characterizing intercalated LDHs and comparing the property changes of different modified asphalts before and after TFOT and UV aging, the following conclusions were drawn:

1. Different antioxidant intercalated LDHs were prepared by the ion exchange method. The d_{003} diffraction peaks of the LDHs migrated to the smaller angle direction after intercalation, indicating that the antioxidant molecules entered the interlayer of the LDHs. FTIR spectra confirmed that the absorption peak of CO_3^{2-} of the LDHs disappeared, and the characteristic peak of antioxidant molecules appeared after intercalation. The antioxidants did not decompose after the intercalation.
2. The LDHs after antioxidant intercalation had good ultraviolet absorption capacity, certain reflection ability, and good free radical scavenging ability. Among the three kinds of antioxidant intercalated LDHs, LDHs-3 had the best free radical scavenging effect.
3. The addition of different LDHs modifiers decreased the penetration and ductility and increased the softening point and viscosity of the asphalt binders. The three kinds of antioxidant intercalated LDHs had less impact on the physical properties of asphalt compared to LDHs, and LDHs-3 had the least impact on the asphalt physical properties.
4. The intercalation of antioxidants significantly improved the storage stability of LDHs-modified asphalt, indicating that the antioxidant intercalated LDHs had better compatibility with asphalt than LDHs. LDHs-3 had the best compatibility with asphalt.
5. The antioxidant intercalated LDHs could simultaneously enhance the thermal oxidation and UV aging resistances of the asphalt binders. LMB-1222 showed the best anti-thermal oxidation aging performance, while LMB-3 had the best anti-UV aging performance.
6. LMB-1222 can be used to enhance the thermal oxidation aging resistance of asphalt binders with high viscosity and high mixing temperatures, while LDHs-3 can be used to enhance the UV aging resistance of asphalt binders used in the areas with high UV radiation intensity. A combination of LDHs-3 and LMB-1222 will bring about the best thermal oxidation aging and UV aging resistance enhancements on asphalt binders.

The output of this research will lay the foundation for developing aging-resistant asphalt and improving the durability of asphalt pavement. The long-term anti-aging effects of the antioxidant intercalated LDHs will be explored in future research.

Author Contributions: Methodology, Q.L.; Formal analysis, Q.L. and J.L.; Investigation, J.L. and S.C.; Writing—original draft, J.L. and S.C.; Supervision, Q.L.; Project administration, Q.L. All authors have read and agreed to the published version of the manuscript.

Funding: The work presented in this paper was financially supported by the National Natural Science Foundation of China (No. 52378462) and the State Key Laboratory of Silicate Materials for Architectures (Wuhan University of Technology) (SYSJJ2023-07).

Data Availability Statement: Data are contained within the article.

Conflicts of Interest: The authors declare no conflicts of interest.

References

1. Song, S.; Wang, L.; Fu, C.; Guo, M.; Jiang, X.; Liang, M.; Yan, L. Study on the Aging Behavior of Asphalt Binder Exposed to Different Environmental Factors. *Appl. Sci.* **2023**, *13*, 12651. [[CrossRef](#)]
2. Ma, F.; Wang, Y.; Fu, Z.; Tang, Y.; Dai, J.; Li, C.; Dong, W. Thermal ageing mechanism of a natural rock-modified asphalt binder using Fourier Transform Infrared Spectroscopy analysis. *Constr. Build. Mater.* **2022**, *335*, 127494. [[CrossRef](#)]
3. Tauste-Martínez, R.; Navarro, F.M.M.; Sol-Sánchez, M.; Rubio-Gamez, M.C. Understanding the bitumen ageing phenomenon: A review. *Constr. Build. Mater.* **2018**, *192*, 593–609. [[CrossRef](#)]
4. Sun, G.; Li, B.; Sun, D.; Yu, F.; Hu, M. Chemo-rheological and morphology evolution of polymer modified bitumens under thermal oxidative and all-weather aging. *Fuel* **2021**, *285*, 118989. [[CrossRef](#)]
5. Xu, G.; Wang, H. Molecular dynamics study of oxidative aging effect on asphalt binder properties. *Fuel* **2017**, *188*, 1–10. [[CrossRef](#)]
6. Jain, S.; Sharma, M. Stability of biodiesel and its blends: A review. *Renew. Sustain. Energy Rev.* **2010**, *14*, 667–678. [[CrossRef](#)]
7. Hu, D.; Gu, X.; Wang, G.; Zhou, Z.; Sun, L.; Pei, J. Performance and mechanism of lignin and quercetin as bio-based anti-aging agents for asphalt binder: A combined experimental and ab initio study. *J. Mol. Liq.* **2022**, *359*, 119310. [[CrossRef](#)]
8. Dehouche, N.; Kaci, M.; Mokhtar, K.A. Influence of thermo-oxidative aging on chemical composition and physical properties of polymer modified bitumens. *Constr. Build. Mater.* **2012**, *26*, 350–356. [[CrossRef](#)]
9. Malinowski, S.; Bandura, L.; Wozzuk, A. Influence of atmospheric oxygen on the structure and electronic properties of bitumen components—A DFT study. *Fuel* **2022**, *325*, 124551. [[CrossRef](#)]

10. Xu, S. Preparation, Performance and Modification Mechanism of Organic Intercalated LDHs Modified Bitumen. Ph.D. Thesis, Wuhan University of Technology, Wuhan, China, 2016.
11. Farrokhzade, F.; Sabouri, M.; Tabatabaee, N. Aging characteristics of neat and modified asphalt binders based on rheological evaluations at intermediate temperatures. *Constr. Build. Mater.* **2022**, *322*, 126387. [[CrossRef](#)]
12. Li, J.; Yang, J.; Liu, Y.; Zhao, Z.; Tang, X.; Luo, J.; Muhammad, Y. Fabrication of IPDI-LDHs/SBS modified asphalt with enhanced thermal aging and UV aging resistance. *Constr. Build. Mater.* **2021**, *302*, 124131. [[CrossRef](#)]
13. Malinowski, S. Aromatisation process as part of bitumen ageing in the light of electronic structure and further oxidation of its components. *Constr. Build. Mater.* **2023**, *366*, 130198. [[CrossRef](#)]
14. Hu, J.; Wu, S.; Liu, Q.; Hernández, M.I.G.; Wang, Z.; Nie, S.; Zhang, G. Effect of ultraviolet radiation in different wavebands on bitumen. *Constr. Build. Mater.* **2018**, *159*, 479–485. [[CrossRef](#)]
15. Zeng, W.; Wu, S.; Pang, L.; Chen, H.; Hu, J.; Sun, Y.; Chen, Z. Research on Ultra Violet (UV) aging depth of asphalts. *Constr. Build. Mater.* **2018**, *160*, 620–627. [[CrossRef](#)]
16. Wu, S.; Zhao, Z.; Xiao, Y.; Yi, M.; Chen, Z.; Li, M. Evaluation of mechanical properties and aging index of 10-year field aged asphalt materials. *Constr. Build. Mater.* **2017**, *155*, 1158–1167. [[CrossRef](#)]
17. Shi, K.; Ma, F.; Liu, J.; Fu, Z.; Song, R.; Yuan, D.; Li, C. Rejuvenation effect of aged SBS-modified asphalt utilizing molecule analysis. *J. Clean. Prod.* **2023**, *405*, 136964. [[CrossRef](#)]
18. Cong, P.; Wang, X.; Xu, P.; Liu, J.; He, R.; Chen, S. Investigation on properties of polymer modified asphalt containing various antiaging agents. *Polym. Degrad. Stab.* **2013**, *98*, 2627–2634. [[CrossRef](#)]
19. Zhang, P.; Guo, Q.; Tao, J.; Ma, D.; Wang, Y. Aging Mechanism of a Diatomite-Modified Asphalt Binder Using Fourier-Transform Infrared (FTIR) Spectroscopy Analysis. *Materials* **2019**, *12*, 988. [[CrossRef](#)]
20. Wu, W.; Li, L.; Yu, J.; Xu, S.; Zhang, C.; Xue, L. Investigation on thermo-oxidative aging properties of asphalt binder with hindered phenolic antioxidant. *J. Test. Eval.* **2018**, *46*, 624–630. [[CrossRef](#)]
21. Ouyang, C.; Wang, S.; Zhang, Y.; Zhang, Y. Improving the aging resistance of asphalt by addition of Zinc dialkyldithiophosphate. *Fuel* **2006**, *85*, 1060–1066. [[CrossRef](#)]
22. Liu, G.; Wu, S.; van de Ven, M.; Molenaar, A. Structure and artificial ageing behavior of organo montmorillonite bitumen nanocomposites. *Appl. Clay Sci.* **2013**, *72*, 49–54. [[CrossRef](#)]
23. Wang, D.; Liu, Q.; Yang, Q.; Tovar, C.; Tan, Y.; Oeser, M. Thermal oxidative and ultraviolet ageing behavior of nano-montmorillonite modified bitumen. *J. Road Mater. Pavement Des.* **2021**, *22*, 121–139. [[CrossRef](#)]
24. Zhang, H.; Yu, J.; Kuang, D. Effect of expanded vermiculite on aging properties of bitumen. *Constr. Build. Mater.* **2012**, *26*, 244–248. [[CrossRef](#)]
25. Zhang, H.; Jia, X.; Yu, J.; Xue, L. Effect of expanded vermiculite on microstructures and aging properties of styrene-butadiene-styrene copolymer modified bitumen. *Constr. Build. Mater.* **2013**, *40*, 224–230. [[CrossRef](#)]
26. Zhang, H.-L.; Su, M.-M.; Zhao, S.-F.; Zhang, Y.-P.; Zhang, Z.-P. High and low temperature properties of nano-particles/polymer modified asphalt. *Constr. Build. Mater.* **2016**, *114*, 323–332. [[CrossRef](#)]
27. Xu, X.; Guo, H.; Wang, X.; Zhang, M.; Wang, Z.; Yang, B. Physical properties and anti-aging characteristics of asphalt modified with nano-zinc oxide powder. *Constr. Build. Mater.* **2019**, *224*, 732–742. [[CrossRef](#)]
28. Chen, S.; Zou, Y.; Liu, Q.; Wu, H.; Wu, S. Synthesis of Hydrotalcite from Phosphate Tailings and Its Effect on the Anti-Ultraviolet Aging Properties of Asphalt Binder. *J. Mater. Civ. Eng.* **2022**, *34*, 04022230. [[CrossRef](#)]
29. Du, L.; Qu, B.; Meng, Y.; Zhu, Q. Structural characterization and thermal and mechanical properties of poly(propylene carbonate)/MgAl-LDH exfoliation nanocomposite via solution intercalation. *Compos. Sci. Technol.* **2006**, *66*, 913–918. [[CrossRef](#)]
30. Xu, S.; Yu, J.; Zhang, C.; Sun, Y. Effect of ultraviolet aging on rheological properties of organic intercalated layered double hydroxides modified asphalt. *Constr. Build. Mater.* **2015**, *75*, 421–428. [[CrossRef](#)]
31. Xu, S.; Yu, J.; Zhang, C.; Yao, T.; Sun, Y. Effect of salicylic acid intercalated layered double hydroxides on ultraviolet aging properties of bitumen. *Mater. Struct.* **2015**, *49*, 1235–1244. [[CrossRef](#)]
32. Chen, S.; Liu, Q.; Wu, H.; Yang, C.; Gong, X.; Wu, S.; Li, Y. Simultaneous enhancement of the thermal oxygen and ultraviolet aging resistance of asphalt by incorporating antioxidant intercalated layered double hydroxide. *Constr. Build. Mater.* **2022**, *349*, 128743. [[CrossRef](#)]
33. *JTG F40-2004*; Technical Specifications for Construction of Highway Asphalt Pavement. Research Institute of Highway, Ministry of Transport: Beijing, China, 2004.
34. Mirwald, J.; Maschauer, D.; Hofko, B.; Grothe, H. Impact of reactive oxygen species on bitumen aging—The Viennese binder aging method. *Constr. Build. Mater.* **2020**, *257*, 119495. [[CrossRef](#)]
35. Yang, T.; Xiao, P.; Zhang, J.; Jia, R.; Nawaz, H.; Chen, Z.; Zhang, J. Multifunctional Cellulose Ester Containing Hindered Phenol Groups with Free-Radical-Scavenging and UV-Resistant Activities. *ACS Appl. Mater. Interfaces* **2018**, *11*, 4302–4310. [[CrossRef](#)] [[PubMed](#)]
36. Zhang, C.; Dong, H.; Wang, T.; Li, Y.; Xu, S.; Zheng, Y.; Que, Y.; Chen, Y. Effect of different organic layered double hydroxides on the anti-aging property of bitumen. *Constr. Build. Mater.* **2023**, *367*, 130316. [[CrossRef](#)]
37. *JTG E20-2011*; Standard Test Methods of Bitumen and Bituminous Mixtures for Highway Engineering. Research Institute of Highway, Ministry of Transport: Beijing, China, 2011.

38. Zhang, C.; Yu, J.; Xu, S.; Xue, L.; Cao, Z. Influence of UV aging on the rheological properties of bitumen modified with surface organic layered double hydroxides. *Constr. Build. Mater.* **2016**, *123*, 574–580. [[CrossRef](#)]
39. Cao, Z.; Hao, Q.; Qu, X.; Qiu, K.; Zhao, R.; Liu, Q. Evolution of Structure and Properties of SBS-Modified Asphalt during Aging Process. *Buildings* **2024**, *14*, 291. [[CrossRef](#)]
40. Omairey, E.L.; Zhang, Y.; Al-Malaika, S.; Sheena, H.; Gu, F. Impact of anti-ageing compounds on oxidation ageing kinetics of bitumen by infrared spectroscopy analysis. *Constr. Build. Mater.* **2019**, *223*, 755–764. [[CrossRef](#)]
41. Cao, Z.; Xue, L.; Wu, M.; He, B.; Yu, J.; Chen, M. Effect of etched Layered double hydroxides on anti ultraviolet aging properties of bitumen. *Constr. Build. Mater.* **2018**, *178*, 42–50. [[CrossRef](#)]
42. Pipintakos, G.; Ching, H.V.; Soenen, H.; Sjövall, P.; Mühlich, U.; Van Doorslaer, S.; Varveri, A.; Bergh, W.V.D.; Lu, X. Experimental investigation of the oxidative ageing mechanisms in bitumen. *Constr. Build. Mater.* **2020**, *260*, 119702. [[CrossRef](#)]
43. Wu, J.; Liu, Q.; Wang, C.; Wu, W.; Han, W. Investigation of lignin as an alternative extender of bitumen for asphalt pavements. *J. Clean. Prod.* **2020**, *283*, 124663. [[CrossRef](#)]

Disclaimer/Publisher’s Note: The statements, opinions and data contained in all publications are solely those of the individual author(s) and contributor(s) and not of MDPI and/or the editor(s). MDPI and/or the editor(s) disclaim responsibility for any injury to people or property resulting from any ideas, methods, instructions or products referred to in the content.